Increased CO_2 modifies the carbon balance and the photosynthetic yield of two common Arctic brown seaweeds: *Desmarestia aculeata* and *Alaria esculenta*

Concepción Iñiguez[1*], Raquel Carmona[1], M. Rosario Lorenzo[1], F. Xavier Niell[1], Christian Wiencke[2], Francisco J. L. Gordillo[1]

1 = University of Malaga, Department of Ecology, Faculty of Sciences, Boulevard Louis Pasteur s/n, 29010 Málaga, Spain. 2 = Alfred-Wegener-Institute; Helmholtz Centre for Marine and Polar Research, Department Functional Ecology; Am Handelshafen 12, D-27570 Bremerhaven, Germany.

Running title: Differential effects of CO_2 on two Arctic seaweeds

*Corresponding author: Concepción Iñiguez

E-mail address: iniguez@uma.es

Phone: +34 952 131844

Fax: +34 952 137386

Abstract

Ocean acidification affects with special intensity Arctic ecosystems, being marine photosynthetic organisms a primary target, although the consequences of this process in the carbon fluxes of Arctic algae are still unknown. The alteration of the cellular carbon balance due to physiological acclimation to an increased CO_2 concentration (1300 ppm) in the common Arctic brown seaweeds *Desmarestia aculeata* and *Alaria esculenta* from Kongsfjorden (Svalbard) was analysed. Growth rate of *D. aculeata* was negatively affected by CO_2 enrichment while *A. esculenta* was positively affected, as a result of a different reorganization of the cellular carbon budget in both species. *Desmarestia aculeata* showed increased respiration, enhanced accumulation of storage biomolecules and elevated release of dissolved organic carbon, whereas *A. esculenta* showed decreased respiration and lower accumulation of storage biomolecules. Gross photosynthesis (measured both as O_2-evolution and ^{14}C-fixation) was not affected in any of them, suggesting that photosynthesis was already saturated at normal CO_2 conditions and did not participate in the acclimation response. However, electron transport rate changed in both species in opposite directions, indicating different energy requirements between treatments and species-specificity. High CO_2 levels also affected the N-metabolism, and ^{13}C isotopic discrimination values from algal tissue pointed to a deactivation of carbon concentrating mechanisms. Since increased CO_2 has the potential to modify physiological mechanisms in different ways in the species studied, it is expected that this may lead to changes in the Arctic seaweed community, which may propagate to the rest of the food web.

Keywords: carbon concentrating mechanisms, growth, macroalgae, ocean acidification, photosynthesis, respiration.

Introduction

The atmospheric concentration of CO_2 has increased by 40% since pre-industrial times due to anthropogenic activities, causing rapid changes in the Earth's climate system, and predictions state that the current partial pressure of CO_2 (pCO_2) of 390 µatm will be exceeded more than twice by the year 2100 (IPCC 2013). One of the main consequences of this phenomenon is ocean acidification (OA), which consists of an increase in CO_2 dissolved in the upper layers of the ocean with a concomitant reduction in the pH, as well as a decrease in CO_3^{2-} concentrations (Doney et al. 2009). Consequently, the ocean has absorbed more than 30% of the emitted anthropogenic CO_2 and the pH of ocean surface water has decreased by 0.1 since the beginning of the industrial era (IPCC 2013). Model simulations further predict that the Arctic will experience the greatest acidification within the global ocean, with pH decreasing by 0.45 units in the present century, a change that is amplified by more than 20% due to freshening and increased carbon dissolution in response to sea ice retreat (Steinacher et al. 2009). Therefore, Arctic marine biota faces a surplus of unprecedented challenges that are beyond what science can document based on available data (Wassmann et al. 2011).

The Arctic coastal environment is characterized by relatively constant and near-freezing water temperatures and strong seasonal variations in light and nutrient availability (Hop et al. 2002). The mid-sublittoral zone at Kongsfjorden (Spitsbergen) is dominated by kelp beds down to at least 10 m depth, which have a dominant role in carbon fluxes at a regional scale, characterized by high biomass areas (up to 21 kg wet mass m^{-2}; Hop et al. 2002, 2012). *Alaria esculenta* is one of these dominating kelps together with *Laminaria digitata, Saccharina latissima* and the kelp-like species *Saccorhiza dermatodea*. Other brown seaweeds like *Desmarestia aculeata* appear as undergrowth species, sometimes forming a separate belt between the mid- and low sublittoral (Wiencke et al. 2004; Hop et al. 2012).

Macroalgae fix inorganic carbon mainly through the enzyme Ribulose-1,5-bisphosphate carboxylase/oxygenase (Rubisco), which can only use CO_2 as inorganic carbon substrate for the carboxylase reaction. Initially, the increase in CO_2 was supposed to favour photosynthesis in macroalgae, taking into account that the majority of their Rubisco is not saturated at present CO_2 concentrations (Raven and Beardall 2003). However, in only few species photosynthesis is dependent on CO_2 passive diffusion (mostly reds), but most seaweeds possess carbon concentrating mechanisms (CCMs), which increase CO_2 concentration around Rubisco (up to 1000 times) via facilitated or active transport of CO_2 and/or HCO_3^- inside the cell, therefore saturating their photosynthetic carbon demand (Giordano et al. 2005). Thus, photosynthesis of macroalgae with CCMs was supposed not to be affected by the increase in CO_2 (Israel and Hophy 2002); nevertheless, these mechanisms are energetically expensive and their partial deactivation at higher concentration of CO_2 could decrease the energetic demand, as it has been previously shown in different algal species (Gordillo et al. 2001; Hurd et al. 2009; Cornwall et al. 2012). In this way, this energy could be invested in other processes such as assimilation of other nutrients, resulting in an increase in the growth rate of those species (Gordillo et al. 2001), although some of them do not show any deactivation of CCMs in response to increased CO_2 (Zou and Gao 2009; Zou et al. 2011a).

A rise in CO_2 concentration does not always have a positive consequence in macroalgae, as this process causes a decreased saturation state of $CaCO_3$ which could make calcification more difficult for marine

calcifying seaweeds (Hall-Spencer et al. 2008); but there are also reports of a negative effect of increased CO_2 on growth rate in non-calcifying ones (Mercado et al. 1999; Israel and Hophy 2002; Gutow et al. 2014), probably due to an inability to compensate carbon fluxes with the metabolism of other nutrients or due to a negative effect on the physiology caused by the decrease in the external pH.

Since the effect of OA on growth and photosynthetic performance has shown to be species-specific, with some species benefitting and some others showing inhibition or no response, it is supposed that OA might promote changes at the community level (Olischläger and Wiencke 2013).

The knowledge about the effects of a rise in CO_2 in the carbon budget of a thallus is scarce, with most of the studies focusing mainly on inorganic carbon acquisition, photosynthetic performance and growth, but less attention has been given to carbon losses due to respiration and organic carbon release, or carbon accumulation in storage biomolecules as another carbon sink, hence, closing the carbon balance. Previous evidence of a decrease in respiration rate by high CO_2 concentrations has been reported in vascular plants (Bunce and Caulfield 1991; Azcón-Bieto et al. 1994) and in the chlorophyte *Ulva rigida* (Gordillo et al. 2001), in the latter allowing an increase in growth rate despite the unchanged photosynthetic rate; while other macroalgal species did not change their respiration rate when exposed to increased CO_2 (Zou and Gao 2009; Zou et al. 2011a; Suárez-Álvarez et al. 2012).

Additionally, the release of dissolved organic carbon (DOC) is usually considered one of the main carbon and energy losses in algae, together with respiration and grazing, and has been frequently used to explain the uncoupling between assimilated carbon and biomass in studies about CO_2 effects on algae (Riebesell et al. 2007; Hopkinson et al. 2010). This mechanism is suggested to account for the maintenance of the internal C:N ratio as has been shown for the cyanobacterium *Spirulina platensis* (Gordillo et al. 1999), for *U. rigida* (Gordillo et al. 2001) and in coastal phytoplankton (Sobrino et al. 2014).

Despite the high research interest in Arctic ecosystems due to its prime affection by global change, little is known about the consequences of OA on the carbon fluxes in Arctic seaweeds. These organisms commonly dominate the coastal systems, but there is a lack of knowledge about the cellular carbon budget and the competitive advantages and disadvantages triggered by increasing CO_2 levels. Some Arctic species (kelps and other brown seaweeds) have shown to possess nutritional strategies that allow them to cope with the long periods of darkness in winter and nutrient depletion in summer, by accumulating photosynthates during summer which support new growth during N-sufficient winter (Chapman and Lindley 1980; Korb and Gerard 2000; Wiencke et al. 2007). Therefore, carbon accumulation in storage biomolecules must be a relevant process in Arctic brown seaweeds but it is unknown to what extent they are going to be affected by OA. Information on winner and loser species is certainly lacking. This is especially relevant as it is expected that changes in the Arctic macroalgal communities will propagate along the food web.

The aim of this study was to determine the physiological acclimation strategies of two representative species of the Arctic macroalgal community, *D. aculeata* and *A. esculenta*, to the increase in CO_2 concentration expected in near-future scenarios. The results provide new highlights on the knowledge of

cellular carbon flux, physiology and photochemical performance in Arctic seaweeds as they are affected by OA.

Materials and methods

Plant material

Two major Arctic brown seaweeds were examined in this study: *D. aculeata* (L.) J. V. Lamour (Desmarestiales, Phaeophyceae) and *A. esculenta* (L.) Greville (Laminariales, Phaeophyceae). The experiments were carried out in July 2013 under laboratory conditions in Kongsfjorden (79 ºN, 11 ºE; Spitsbergen, Svalbard; see Fig. 1). The specimens were collected by divers at 5-6 m (*D. aculeata*) and 8-10 m (*A. esculenta*) depth in Hansneset and carried immediately to the laboratory in black plastic bags. For *A. esculenta*, young sporophytes were selected (length: 10-15 cm), but for *D. aculeata* only mature sporophytes were available. Thus, we used the whole thallus of *A. esculenta*, but for *D. aculeata* we previously cut the apical parts of different thalli, just below the meristematic zone, where the active growth occurs. Thalli were kept in 100 L containers under continuous seawater circulation at around 4ºC for 24 h before the experiments. Visually healthy thalli, free from macroscopic epibiota were chosen for the experiments.

Experimental setup

Algal specimens were cultured for 7 days at two different dissolved CO_2 concentrations, 390 and 1300 ppm, by aerating the medium with regular air or CO_2-enriched air (final aeration of 1 L min^{-1}). For the high CO_2 treatment, a stream of pure CO_2 was mixed with regular air, yielding CO_2-enriched air of approximately 1300 ppm, and was continuously controlled with a Carbon Dioxide Sensor (*AirSense* Model 310e, Digital control Systems, Inc., USA). The two CO_2-conditions were verified by measuring seawater pH (NBS-scale) and determining total alkalinity (TA) by potentiometric titrations (Gran 1952) every other day; then, CO_2 speciation was calculated using the CO2calc Package (Robbins et al. 2010), with the CO_2 acidity constants of Mehrbach et al. (1973) and the CO_2 solubility coefficient of Weiss (1974).

Cultures started after 3 days of pre-acclimation to the two conditions to avoid the interference of rapid and transient responses to increased CO_2 levels. As shown in previous studies, a total of 10 days of exposure to different CO_2 concentrations (3 days of pre-incubation + 7 days of incubation) would be enough time for acclimation in seaweeds (Mercado et al. 1999; Andría et al. 2001; Zou 2005). Experiments were carried out in a temperature-controlled room (4 ± 0.5°C) with a 20:4 h light:dark photoperiod (as a proxy to conditions in the collection site), using 1.5 L perspex cylinders with 0.2 µm-filtered natural seawater (FSW) enriched with nutrients, following a modified, buffer-free recipe of Provasoli (1968). A constant photon fluence rate (PFR) of 25-30 µmol photons m^{-2} s^{-1} at the surface of the FSW in the cylinder was provided by daylight fluorescent lamps (L36W/954 Osram, Germany). PFR was measured by means of a quantum flat head PAR sensor (LI-190) connected to a radiometer (LiCor-250A Light Meter; Li-Cor Biosciences, Lincoln, USA). It corresponded to 65-70 µmol photons m^{-2} s^{-1} inside the water in the middle of the cylinder as measured with a spherical sensor (US-SQS/L, Walz,

Germany). For each cylinder about 1 g initial fresh weight (FW) of alga was used. Four cylinders containing each of them 4-5 independent specimens were used for each treatment. The physiological measurements described below were applied to fresh material taken directly from each cylinder at the end of the 7-days incubation period. Biochemical composition was analysed from freeze-dried material stored at -80 ºC.

Determination of the growth rate

Thallus growth was calculated by the difference between initial and final FW in each cylinder. Growth rate was estimated by fitting the exponential function, as proposed by Lüning (1985):

$P_t = P_0 \cdot e^{rt}$

where r represents the intrinsic growth rate (% d^{-1}), P_t is the final fresh weight, P_0 the initial fresh weight, and t the elapsed time in days.

Chlorophyll fluorescence

Optimal quantum yield for PSII fluorescence (F_v/F_m) was measured by means of a pulse amplitude modulated fluorimeter using a Mini-PAM (Walz, Effeltrich, Germany) after 15 min of incubation in darkness, as described by Schreiber et al. (1986). Immediately afterwards, rapid light curves were measured using the same device, where the effective quantum yield of PSII ($\Phi_{PSII} = \Delta F/F_m'$) was estimated for 8 different white light irradiances provided by the internal halogen lamp. According to Genty et al. (1989), F_v is the maximal variable fluorescence of a dark-adapted sample, F_m the fluorescence intensity with all PSII reaction centres closed, F the fluorescence at any time during induction and F_m' the light-saturated fluorescence. The electron transport rate between PSII and PSI (ETR) at each irradiance was calculated as:

$$ETR = \Phi_{PSII} \cdot PFR \cdot 0.5 \cdot A$$

where 0.5 stands for the assumption of equal contribution of excitons from PSI and PSII, and A is the thallus absorptance. The parameter A was estimated according to Beer et al. (2000), as the fraction of incident photons of photosynthetic active radiation (PAR) absorbed by the thallus:

$$A = 1 - T$$

where T is the transmittance, and assuming no significant reflectance. The transmittance was determined by comparing readings from a quantum flat head PAR sensor (LI-190, Li-Cor Biosciences, Lincoln, USA) connected to a LiCor radiometer, with and without the thallus placed in the surface of the sensor, with a white led-lamp irradiating perpendicularly at a fixed distance.

ETR vs. irradiance curves were fitted to the non-linear least-squares regression model by Eilers and Peeters (1988) using the Solver function of Excel (Microsoft, Redmond, U.S.A.) in order to obtain photosynthetic parameters: maximum electron transport rate (ETR_{max}), the initial slope of the curve related to the photosynthetic light-harvesting efficiency (α), the light requirement for saturating

photosynthetic rate (E_k) which is given as the intercept between α and ETR_{max}, and the irradiance at which chronic photoinhibition begins (E_{0pt}).

All measurements were performed for each treatment (n = 4) after 7 days of cultivation using sterile-FSW pre-equilibrated at either 390 or 1300 ppm CO_2.

Photosynthetic rates by O_2 evolution and ^{14}C fixation

Pieces of blade of 50-100 mg FW used for measuring photosynthesis (by ^{14}C fixation and oxygen evolution) and respiration were cut the day before measurements to avoid wound-healing interference. Sterile-FSW pre-equilibrated at either 390 or 1300 ppm CO_2 was used for all measurements of photosynthesis/respiration.

- Oxygen evolution

Net photosynthesis (NPS) under culture PFR provided by white light led-lamps, as well as dark respiration were estimated by oxygen evolution using a Clark-type oxygen electrode (5331; Yellow Spring Instruments, Ohio, USA) in 8-ml custom-made transparent Plexiglas chambers at 4 ± 0.2 °C. The water in the chambers was continuously stirred. Rate measurements were made at 15 min intervals.

- Inorganic ^{14}C fixation

Measurements were based on the protocol proposed by Kremer and Küppers (1977). Samples were allowed to photosynthesize in a $H^{14}CO_3^-$ (Perkin Elmer, USA) medium, or to assimilate ^{14}C in darkness (as a control of light-independent carbon fixation). Thalli were placed in 8 ml septum-sealed glass vials filled with sterile FSW in a custom-made transparent Plexiglas container connected to a thermo-regulated water bath at 4 ± 0.2°C, under culture PFR and with continuous homogenisation of the medium by a magnetic stirrer. A pre-acclimation period of 15 min in light for steady photosynthesis measurements and of 30 min in darkness for the dark control was applied before adding the $H^{14}CO_3^-$ solution. Subsequently, an aliquot of the $H^{14}CO_3^-$ stock was injected through the septum to yield a final specific activity of ~ 0.25 μCi μmol C^{-1}, and thalli were incubated during 30 min either in light or darkness. This incubation time was chosen in pilot experiments, trying to find the lowest time for the incubation which maintains enough sensitivity. After the incubation period, thalli were immediately rinsed in unlabelled medium, blotted, submersed in liquid nitrogen to stop reactions, and settled in 20-ml scintillation vials containing 400 μl of HNO_3 (68%); then, after 10 min at 50ºC, vials were left uncapped in an orbital shaker inside a fumehood until complete tissue solubilisation.

The equivalent carbon fixation rates were determined by measurements of acid-stable ^{14}C fixation after the addition of 10 ml of scintillation cocktail (Insta-gel, Perkin Elmer), using a liquid scintillation counter (TriCarb 2910, Perkin Elmer) with automatic quench correction, and referred to the total inorganic carbon content of the incubation media used. Activity levels of dark controls were subtracted from light ^{14}C-fixation measurements. For the calculation of the carbon fixation rate it was assumed that the uptake of ^{14}C is 5% slower than ^{12}C (based on Steeman-Nielsen 1952).

Total carbon and nitrogen content

Total internal C and N contents were determined from freeze-dried tissue samples after homogenisation, using a C:H:N elemental auto-analyser (Perkin-Elmer 2400CHN) by DOI method (Kristensen and Andersen 1987).

Stable Isotopic determination

The abundance of ^{13}C relative to ^{12}C in plant samples (c.a. 30 mg of dry mass) was determined by mass spectrometry using a DELTA V Advantage (Thermo Electron Corporation, USA) Isotope Ratio Mass Spectrometer (IRMS) connected to a Flash EA 1112 CNH analyser. The ^{13}C isotopic discrimination in the algal samples ($\delta^{13}C_{alga}$) was expressed in the unit notation as deviations from the $^{13}C/^{12}C$ ratio of the Pee-Dee Belemnite $CaCO_3$ (PDB) calculated according to:

$$\delta^{13}C\ (‰) = [(^{13}C/^{12}C)_{sample}/(^{13}C/^{12}C)_{PDB} - 1] \cdot 10^3$$

To determine isotopic composition of dissolved inorganic carbon ($\delta^{13}C_{DIC}$), 20 ml of FSW from each cylinder was filtered (Whatman GF/F), fixed and stored in septum-sealed glass vials without leaving a head-space. Measurements of $\delta^{13}C_{DIC}$ were performed with the same IRMS mentioned above connected to a GasBench II (Thermo Electron Corporation) system.

The $\delta^{13}C_{alga}$ was corrected with the $\delta^{13}C_{DIC}$ values from the medium, since the CO_2-source used in the experiment for the CO_2-enriched treatment came from previously fixed CO_2 which had been already discriminated.

DOC and POC

Samples for the determination of dissolved organic carbon (DOC) present in the growth medium were taken at the beginning and at the end of the incubation period and analysed by an automated system (TOC-L CSN, Shimadzu Corporation, Kyoto, Japan) according to the manufacturer's protocols after filtration (Whatman GF/F). The filter was dried overnight at 80°C and used for the determination of particulate organic carbon (POC) using the same elemental auto-analyser described above.

Data analyses

Replicate measurements (n = 4 independent thalli) were tested for significance of differences ($P < 0.05$) promoted by differences in CO_2 enrichment for each species using t-tests. All statistical analyses were performed using the SigmaPlot 11.0 statistical software (Systat Software Inc., USA).

Results

Table 1 shows the averaged values of the different variables of the seawater carbonate system in both CO_2 treatments, along the culture period. When pH was changed from 8.18 to 7.72 by aerating with CO_2-enriched air, dissolved inorganic carbon (DIC), dissolved CO_2 and HCO_3^- increased by 6%, 204% and 8%, respectively, and CO_3^{2-} decreased by 63%, while TA showed no significant differences between low- and high-CO_2 cultures.

Growth rate was significantly affected by the increase in dissolved CO_2 in both species, but not in the same direction. Rather, at high CO_2, growth rate of *D. aculeata* decreased by 82 % from 1.1 to 0.2 % d^{-1} while in *A. esculenta* it increased by 34 % from 7.2 to 9.7 % d^{-1} (Fig. 2). It must also be noted that *A. esculenta* exhibited a much higher growth rate than *D. aculeata* at both CO_2 treatments.

In contrast to growth rate, gross oxygen production as well as C fixation rates did not show any significant differences between treatments for any of the two species (Fig. 3). Respiration rate decreased by 50% from 10.6 to 5.3 μmol O_2 g FW^{-1} h^{-1} in *A. esculenta* at high CO_2 conditions, while it increased in *D. aculeata* from 3.1 to 4.9 μmol O_2 g FW^{-1} h^{-1}. *Desmarestia aculeata* had a slight, but significantly lower net oxygen production rate at high CO_2, while *A. esculenta* exhibited no significant differences in net oxygen production rate. DOC release rate increased significantly in both species at high CO_2, especially in *D. aculeata*, with a value 5 times higher than at normal CO_2 conditions, from 0.1 to 0.49 μmol C g FW^{-1} h^{-1} in *D. aculeata* and from 0.23 to 0.57 μmol C g FW^{-1} h^{-1} in *A. esculenta*, while POC release rate did not show any significant differences between treatments (Fig. 4).

The relative contribution of the processes affecting the cellular carbon budget is shown in Fig. 5. Each process was recalculated to account for the organic C produced or consumed during the 7 days of cultivation for each cylinder (replicate), and is expressed as a percentage of the total amount of C fixed during that period (considering ^{14}C fixation measurements as gross photosynthesis), which is invested in either respiration, new biomass production (growth), carbon accumulation in storage biomolecules not invested in growth, or DOC and POC released to the external medium. A constant light-dependent C fixation rate during the cultivation period and a constant respiration rate during light and dark periods over the 7 days of cultivation were assumed. The quantity of C accumulated in storage molecules was calculated as the difference in the total C-content of algal biomass (data from Table 4), corrected by the integrated DW, between the initial and the final time of the incubation period. In *D. aculeata*, the percentage of C fixed invested in growth strongly decreased at high CO_2 (from 25 to 5% of total carbon fixed) at the expense of an increase in respiration, organic carbon accumulation and DOC release; whereas *A. esculenta* increased growth at high CO_2 (with an increment of around 15% of total carbon fixed) as a result of a decrease in respiration and in organic carbon accumulation.

Respect to the operation of photosynthesis, rapid light curves indicated a significant lower maximum electron transport rate (ETR_{max}) at elevated CO_2 conditions in *D. aculeata* (by 30%), and a 35% higher photosynthetic efficiency (α) and 60% higher ETR_{max} at high CO_2 in *A. esculenta* (Table 2). Electron transport rate at 30 μmol photons m^{-2} s^{-1} (ETR_{30}), resembling culture conditions, showed significant differences between treatments in both species, with an increase of 45 % in *A. esculenta* and a decrease of 15% in *D. aculeata* at increased CO_2, respect to normal CO_2 conditions. There was also a significant increase in the saturating irradiance (E_k) and the irradiance at which chronic photoinhibition begins (E_{0pt}) of about 25% for *A. esculenta* at this condition, while *D. aculeata* did not show any significant differences in those parameters. Optimal quantum yield for PSII fluorescence (F_v/F_m) was not affected by CO_2 in any of the species, showing common optimal values for brown algae, thus indicating that thalli from both species and treatments were in an overall healthy state.

289 The photosynthetic quotient (PQ), calculated as the molar ratio of the rate of gross oxygen production to
290 the rate of carbon dioxide fixation, was significantly lower at high CO_2 in *A. esculenta*, showing a
291 decrease from 1.92 to 1.41, but it was not affected by CO_2 in *D. aculeata*, with values around 1.34 (Table
292 3).

293 The ^{13}C isotopic discrimination in the algal samples ($\delta^{13}C_{alga}$), which was corrected with the isotopic
294 composition of DIC in the medium, was significantly lower at high CO_2 in both species, with a decrease
295 from -19.2 to -23.5‰ for *D. aculeata* and a decrease from -21.8 to -28.7‰ for *A. esculenta* (Table 4).
296 FW:DW ratio significantly increased in *A. esculenta* at high CO_2, indicating a higher water content in this
297 condition, while it did not change in *D. aculeata*. Elevated CO_2 levels affected the nitrogen metabolism of
298 these species in opposite ways, decreasing the percentage of internal N in *D. aculeata* and increasing it in
299 *A. esculenta*, whereas the percentage of internal C, as well as the C:N ratio, slightly decreased at high
300 CO_2 only in *A. esculenta* (Table 4). Therefore, N- metabolism was enhanced at increased CO_2 conditions
301 in *A. esculenta*, but not in *D. aculeata.*

302 **Discussion**

303 The increase in dissolved CO_2 concentration has shown the potential to change the carbon yield and fate
304 in common seaweed species of the Arctic in different ways. The negative effect of elevated CO_2 in the
305 growth rate of *D. aculeata* has also been observed in other seaweeds such as the rhodophytes *Hypnea*
306 *musciformis* (Israel and Hophy 2002), *Porphyra leucosticta* (Mercado et al. 1999) and *Porphyra linearis*
307 (Israel et al. 1999), and the phaeophytes *Fucus vesiculosus* (Gutow et al. 2014) and *S. latissima* (Swanson
308 and Fox 2007). As reason for this effect, the pH sensitivity of the specific CCMs of *Porphyra* species has
309 been invoked (Moulin et al. 2011). For *S. latissima*, likewise, the authors proposed that the CCMs of this
310 species allow for optimal photosynthesis at high seawater pH (Axelsson et al. 2000). Another possibility
311 for the decrease in growth rate at high CO_2 conditions could be a lack of ability to equilibrate carbon
312 fluxes with the metabolism of other nutrients such as N, as indicated by a lower total N- content, or a lack
313 or malfunction of internal pH regulation. However, in our experiment *D. aculeata* seemed not to be
314 photochemically stressed as revealed by F_v/F_m values, unlike *P. leucosticta* (Mercado et al. 1999) and *H.*
315 *musciformis* (Israel and Hophy 2002), which showed clear evidence of photochemical stress at increased
316 CO_2 levels.

317 On the other hand, the positive effect of elevated CO_2 in the growth rate of *A. esculenta* has also been
318 observed in many species of seaweeds such as the rhodophytes *Lomentaria articulata* (Kübler et al.
319 1999), *Hypnea spinella* (Suárez-Álvarez et al. 2012) and *Neosiphonia harveyi* (Olischläger and Wiencke
320 2013), the chlorophyte *U. rigida* (Gordillo et al. 2001) and the brown turf-forming alga *Feldmannia* sp.
321 (Russell et al. 2009). This is the expected acclimation response of a photosynthetic organism to increased
322 CO_2 when photosynthesis is not saturated at normal DIC level. Nevertheless, *A. esculenta* and *D.*
323 *aculeata* did not change the C fixation rate under this condition (see Fig. 3c), indicating that their
324 photosynthesis is already saturated at normal CO_2 levels, so the effect of CO_2 on growth does not
325 correlate with the absence of effect on gross photosynthesis. The same pattern as in *A. esculenta* was
326 obtained for *U. rigida* (Gordillo et al. 2001), in which the stimulation of growth was not caused by an

increase in the photosynthetic rate; instead, the source of C for the extra biomass production came from the reduction in carbon losses.

DOC release has been proposed as a regulatory mechanism able to respond to the environment (Fogg 1983; Ormerod 1983), which would maintain the metabolic integrity of the cell and would protect the photosynthetic apparatus from an overload of products that cannot be used in growth or stored (Wood and Van Valen 1990). The release of DOC under high CO_2 levels increased in the unicellular green alga *Dunaliella salina* (Giordano et al. 1994) and in the coccolithophorid *Emiliania huxleyi* (Borchard and Engel 2012), while Hopkinson et al. (2010) and Sobrino et al. (2014) found that high CO_2 conditions reduced cellular carbon loss in natural phytoplanktonic communities. Furthermore, DOC release is suggested to act as a mechanism controlling the internal C:N ratio in the cyanobacterium *S. platensis* (Gordillo et al. 1999), in *U. rigida* (Gordillo et al. 2001) and in coastal phytoplankton (Sobrino et al. 2014). In this way, both species of the present study seem to increase the release of DOC at high CO_2 conditions, although the percentage of extracellular release (PER) was always in the range between 0 and 10 % of photosynthetic carbon assimilation (see Fig. 5, d), as it has been shown for healthy growing algae (Sharp 1977; Mague et al. 1980). In *D. aculeata,* the decrease in total N- content at high CO_2 levels, presumably due to a decrease in the assimilation rate of N, could lead to an enhancement in DOC release, thus maintaining the internal C:N ratio. However, in *A. esculenta* the C:N ratio is not maintained between treatments, due to an increase in DOC release at enriched-CO_2 levels together with an enhancement of the uptake and assimilation of N, as is suggested by the higher N- content values.

Changes in dark respiration rates are in accordance with the growth rate response. Previous evidence of the decrease in respiration rate by high CO_2 concentrations has been reported in vascular plants (Bunce and Caulfield 1991; Azcón-Bieto et al. 1994) and in *U. rigida* (Gordillo et al. 2001), although there were no changes in respiration rates in the rhodophytes *P. leucosticta* (Mercado et al. 1999), *H. spinella* (Suárez-Álvarez et al. 2012), *Gracilaria lemaneiformis* (Zou and Gao 2009) and *Hizikia fusiformis* (Zou et al. 2011a). On the contrary, an increase in the respiration rate was recorded in some vascular plants (Davey et al. 2004) and in the diatom *Thalassiosira pseudonana* (Yang and Gao 2012). Stimulation of mitochondrial activity under OA scenarios may be associated to altered proton gradients across the mitochondrial membrane or to pH-dependent changes in the functioning of respiratory enzymes (Amthor 1991). On the other hand, down-regulation of CCMs would leave the cell with excess energy equivalents and so, cells could down-regulate energy production by reducing mitochondrial respiration (Hennon et al. 2014).

Regarding the regulation of the photochemical performance, the significant differences obtained in ETR_{max} between CO_2 treatments in both species could be the result of a change in the number of active reaction centres (see Table 2). Furthermore, the differences obtained in ETR_{30}, in contrast with the absence of effect on gross oxygen production and C fixation in both species, could be due to the alteration in light capture efficiency by PSI and PSII at high CO_2 conditions, as reported by Satoh et al. (2002), along with a change in the photosynthetic pigment content and/or antennae size. In *A. esculenta*, an activation of the cyclic electron flow around PSII as part of a photoprotection strategy at saturating irradiances could explain the increase of ETR_{30} at high CO_2 levels, as suggested for *U. rigida* by Gordillo

et al. (2003) and for *P. tricornutum* by Feikema et al. (2006). In this way, an enhancement of photoprotection mechanisms at high CO_2 in *A. esculenta* could be responsible for the significant increase in E_k and E_{0pt} (Table 2). In *D. aculeata*, increased acidity in the ambient seawater might, to some extent, affect intracellular acid-base balance, and hence, cause a decrease in ETR. The same response has been observed in the haptophyte *Phaeocystis globosa* at the beginning of the acclimation period to elevated CO_2 (Chen et al. 2014), although the photosynthetic efficiency was not affected. It is also necessary to take into account that the calculation of the gross oxygen evolution, which was estimated assuming a constant respiration rate as measured in darkness, could lead to an overestimation since respiration may decrease in light, as it has been previously shown for some seaweeds (Brown and Tregunna 1967, Zou et al. 2011b).

The C fixation rate was not affected by high CO_2 in none of the two species studied, indicating that photosynthesis is carbon-saturated at current CO_2 concentrations due to CCM functioning, as it is suggested by $\delta^{13}C$ isotopic discrimination data. Algae with $\delta^{13}C$ values more negative than -30‰ are unable to increase the pH of seawater above 9.0 (Maberly et al. 1992), which indicates the absence of functional CCMs (photosynthesis relies only on diffusive-CO_2 entry). For *A. esculenta,* Maberly et al. (1992) published a $\delta^{13}C$ value of -17.8‰, while for *D. aculeata* $\delta^{13}C$ values are between -18 and -26‰ (Raven et al. 2002), being these values similar to the ones obtained in the present study at normal CO_2 levels for both species (Table 4).

A significant increase in the carbon isotope discrimination data, i.e. more negative $\delta^{13}C$ values relative to the PDB standard, indicates a deactivation of CCMs in both species at high CO_2 conditions, as reported for other algae (Hurd et al. 2009; Cornwall et al. 2012). In *A. esculenta*, the energy saved due to CCM deactivation could be invested in other processes like assimilation of other nutrients or increasing synthesis of biomolecules, giving an increase in the growth rate, as it has been described for *U. rigida* (Gordillo et al. 2001). In *D. aculeata*, CCM deactivation did not produce an increase in growth rate as ETR_{30} decrease, probably due to the sensitivity of this species to a lower pH. However, $\delta^{13}C$ data should be taken cautiously, since a higher ^{13}C-discrimination not only indicates a higher use of diffusive-CO_2 but also could indicate a higher photosynthetic dependence on the CO_2 supplied from HCO_3^- via external carbonic anhydrase, as this enzyme could also be subjected to kinetic fractionation (Mercado et al. 2009; O'Leary et al. 1992).

Moreover, PQ (which reflects de efficiency of the photochemical reactions from the water reduction occurring in PSII to C fixation) was significantly lower in *A. esculenta* at high CO_2 conditions (Table 3), indicating a lower amount of photosynthetic energy invested in processes other than C fixation, although energy obtained by cyclic electron flow around PSII, which is suggested as a photoprotective mechanism at high CO_2 in this species, is not taken into account by O_2 production. These results are in accordance with the deactivation of CCMs indicated by ^{13}C isotopic discrimination data, although *D. aculeata* did not show significant differences in PQ values, suggesting that the energy saved due to CCM deactivation may be invested in counteracting the external pH reduction (Wu et al. 2010).

403 The carbon balance of *D. aculeata* showed the typical pattern of physiological performance of brown
404 seaweeds in the Arctic during summer. This might explain why the growth is low (25% of total C fixed)
405 and the organic carbon accumulation is high (64%) at control conditions. It has been reported in some
406 species that this pattern is under the control of photoperiodisms or endogenous free-running circannual
407 rhythms entrained by a critical minimum daylength in autumn (Lüning 1991; Schaffelke and Lüning
408 1994; Wiencke et al. 2011), suggesting that the addition of nitrate to summer N- limited brown seaweeds
409 would have only a marginal effect on growth and biochemical composition (Henley and Dunton 1997).
410 Nevertheless, *A. esculenta* responded in a different way, with a high investment of carbon into growth (72
411 % of total C fixed) and a low organic carbon accumulation (14 % of total C fixed) at normal CO_2 levels.
412 It is also possible that the age of the thalli used for the experiment may have influenced this different
413 pattern, together with the morphological differences between both species. Sporophytes of *D. aculeata*
414 have a trichothallic growth in which cell division is restricted to the base of one or several filaments, and
415 the apex of a branch ends with a single filament having a intercalary meristem which produce lateral
416 filaments above and below it (Bold and Wynne 1978); while sporophytes of *A. esculenta* have an
417 intercalary growth with a meristem situated at the juncture of the stipe and the blade. However, it has
418 been shown in other studies that both species could reach similar growth rates (Bischoff and Wiencke
419 1993). Also, young thalli could have a metabolism more focused on growing than mature thalli, although
420 a more plausible explanation for the different growth rates would be that growth in *A. esculenta* is not
421 controlled by this endogenous circannual rhythm or photoperiodism, as demonstrated by Gordillo et al.
422 (2006). The previous study showed a significant change in the nitrate reductase (NR) activity and in the
423 internal N- content at N- enriched conditions compared to N- depleted conditions in the Arctic summer
424 for *A. esculenta*, while *D. aculeata* showed no response in those variables.

425 The decrease in total N- content obtained in *D. aculeata* indicates a lower investment of energy in the N-
426 metabolism, as shown for *Gracilaria tenuistipitata* (García-Sánchez et al. 1994) and *G. lemaneiformis*
427 (Xu et al. 2010), while *A. esculenta* exhibited an increase in total N- content, suggesting a stimulation of
428 N- assimilation, which could be due to a higher synthesis of aminoacids necessary for a higher growth
429 rate. Stimulation of N uptake and assimilation (via increasing NR activity) at high CO_2 conditions has
430 been previously reported in the seaweeds *P. leucosticta* (Mercado et al. 1999), *U. rigida* (Gordillo et al.
431 2001), *Chondrus crispus* and *Cystoseira tamariscifolia* (Olabarria et al. 2012), and in *H. spinella* (Suárez-
432 Álvarez et al. 2012). Moreover, NR activity was significantly enhanced in *A. esculenta* at increased CO_2
433 levels in a similar experiment carried out also in Kongsfjorden (Gordillo et al. unpublished results), which
434 support our results of an increase in total N- content, while NR activity from *D. aculeata* did not change
435 between treatments.

436 Overall, the effect of CO_2 involves a reorganization of the energetic and carbon budget of the cell, and
437 does not reflect a direct effect on photosynthesis in the analysed species, but rather a significant effect on
438 respiration, organic carbon accumulation and DOC release (see Fig. 5), along with an effect on CCMs
439 and N- metabolism, which ultimately determine growth rate. It has been reported that phytoplankton
440 species apparently possess sensory systems that respond to environmental CO_2 concentrations and control

441 the CO_2 acquisition efficiency (Matsuda et al. 2001; Burkhardt et al. 2001), suggesting that CO_2 plays
442 more roles than simply being a substrate for photosynthesis.

443 The sum of the percentages of all processes taken into account in the carbon balance gave a total value
444 higher that 100% for both treatments and species, indicating a possible underestimation of the total C
445 fixed measured by the ^{14}C-method; this could be due to the respiration of some of the ^{14}C-molecules
446 which came from $^{14}CO_2$ already fixed by cells during the 30 min-incubation period, but could also be due
447 to the assumption of a constant respiration rate as measured in darkness, which could lead to an
448 overestimation for the light period as mentioned above.

449 In the CO_2-enriched global scenario predicted, it can be concluded that seaweeds are going to be affected
450 in different species-specific ways. *Alaria esculenta* might be benefitted and *D. aculeata* seems to be a
451 clear loser. As a result, the Arctic seaweed community may shift its relative biomass dominance and the
452 consequences propagate to the rest of the trophic web. Moreover, it is necessary to take into account that
453 interactive effects of CO_2 and other variables such as nutrients, temperature, salinity and irradiance levels
454 may influence their response and, thus, complicate the prediction of implications of OA for seaweeds.

455 Recently, there is a wide discussion regarding the duration of the exposure to increased CO_2 conditions in
456 laboratory experiments. Ten days of incubation have been shown to be enough time to see a physiological
457 acclimation of different species of seaweeds in previous studies, although experiments of longer-term
458 acclimation are also needed to extrapolate their responses to the future environment, as there could be
459 complex effects different from short-term physiological responses. Also, the responses to a more realistic
460 gradual increase in CO_2 are largely unknown (but see Hall-Spencer et al. 2008). However, highly
461 controlled short-term single or multifactorial laboratory experiments, like the present study, are also
462 important in identifying the species' preadapted sensitivities to increasing CO_2 (Roleda and Hurd 2012).

463 **Acknowledgements**

464 This work was performed at the International Arctic Environmental Research and Monitoring Facility at
465 Ny-Ålesund, Spitsbergen, Norway. It was financed by the project CTM2011-24007/ANT from the
466 Spanish Ministry for Science and Innovation. Concepcion Iñiguez and M. Rosario Lorenzo were
467 supported by a FPU grant from the Spanish Ministry for Education. Finally, we thank the AWI diving
468 team and Elisabeth Helmke (AWI) for assistance with ^{14}C counting.

469 **References**

470 Amthor JS (1991) Respiration in a future, higher CO_2 world. Plant Cell Environ 14:13–20
471 Andría JR, Brun FG, Pérez-Lloréns JL, Vergara JJ (2001) Acclimation responses of *Gracilaria sp.*
472 (Rhodophyta) and *Enteromorpha intestinalis* (Chlorophyta) to changes in the external inorganic
473 carbon concentration. Bot mar 44:361–370
474 Axelsson L, Mercado J, Figueroa F (2000) Utilization of HCO_3^- at high pH by the brown macroalga
475 *Laminaria saccharina*. Eur J Phycol 35:53–59

476 Azcón-Bieto J, González-Meler M, Dougherty W, Drake B (1994) Acclimation of respiratory O_2 uptake
477 in green tissues of field-grown native species after long-term exposure to elevated atmospheric
478 CO_2. Plant Physiol 106:1163–1168
479 Beer S, Larsson C, Poryan O, Axelsson L (2000) Photosynthetic rates of *Ulva* (Chlorophyta) measured by
480 pulse amplitude modulated (PAM) fluorescence. Eur J Phycol 35:69–74
481 Bischoff B, Wiencke C (1993) Temperature requirements for growth and survival of macroalgae from
482 Disko Island (Greenland). Helgoländer Meeresunters 47:167–191
483 Bold HC, Wynne MJ (1978) Introduction to the Algae: Structure and Reproduction Prentice-Hall, Inc.
484 Englewood Cliffs, New Jersey
485 Borchard C, Engel A (2012) Organic matter exudation by *Emiliania huxleyi* under simulated future ocean
486 conditions. Biogeosciences 9:3405–3423
487 Brown DL, Tregunna EB (1967) Inhibition of respiration during photosynthesis by some algae. Can J Bot
488 45:1135–43
489 Bunce J, Caulfield F (1991) Reduced respiratory carbon dioxide efflux during growth at elevated carbon
490 dioxide in three herbaceous perennial species. Ann Bot 67:325–330
491 Burkhardt S, Amoroso G, Riebesell U, Sültemeyer D (2001) CO_2 and HCO_3^- uptake in marine diatoms
492 acclimated to different CO_2 concentrations. Limnol Oceanogr 46:1378–1391
493 Chapman ARO, Lindley JE (1980) Seasonal growth of *Laminaria solidungula* in the high Arctic in
494 relation to irradiance and dissolved nutrient concentration. Mar Biol 57:1–5
495 Chen SW, Beardall J, Gao KS (2014) A red tide alga grown under ocean acidification up-regulates its
496 tolerance to lower pH by increasing its photophysiological functions. Biogeosciences Discuss
497 11:6303–6328
498 Cornwall CE, Hepburn CD, Pritchard D, Currie KI, McGraw CM, Hunter KA, Hurd CL (2012) Carbon
499 use strategies in macroalgae: differential responses to lowered pH and implications for ocean
500 acidification. J Phycol 48:137–44
501 Davey PA, Hunt S, Hymus GJ, DeLucia EH, Drake BG, Karnosky DF, Long SP (2004) Respiratory
502 oxygen uptake is not decreased by an instantaneous elevation of [CO_2], but is increased with
503 long-term growth in the field at elevated [CO_2]. Plant Physiol 134:520–527
504 Doney SC, Fabry VJ, Feely RA, Kleypas JA (2009) Ocean acidification: the other CO_2 problem. Ann Rev
505 Mar Sci 1:169–192
506 Eilers PHC, Peeters JCH (1988) A model for the relationship between light intensity and the rate of
507 photosynthesis in phytoplankton. Ecol Modelling 42:199–215
508 Feikema WO, Marosvölgyi MA, Lavaud J, van Gorkom HJ (2006) Cyclic electron transfer in
509 photosystem II in the marine diatom *Phaeodactylum tricornutum*. Biochim Biophys Acta
510 1757:829–34
511 Fogg GE (1983) The ecological significance of extracelular products of phytoplankton. Bot Mar 26:3–14
512 García-Sánchez MJ, Fernández JA, Niell X (1994) Effect of inorganic carbon supply on the
513 photosynthetic physiology of *Gracilaria tenuistipitata*. Planta 194:55–61
514 Genty B, Briantais J, Baker NR (1989) The relationship between the quantum yield of photosynthetic
515 electron transport and quenching of chlorophyll fluorescence. Biochim Biophys Acta 990:87–92

516 Giordano M, Davis S, Bowes G (1994) Organic carbon release by *Dunaliella salina* (Chlorophyta) under
517 different growth conditions of CO_2, nitrogen and salinity. J Phycol 30:249–257
518 Giordano M, Beardall J, Raven JA (2005) CO_2 concentrating mechanisms in algae: mechanisms,
519 environmental modulation, and evolution. Ann Rev Plant Biol 56:99–131
520 Gordillo FJL, Jiménez C, Figueroa FL, Niell FX (1999) Effects of increased atmospheric CO_2 and N
521 supply on photosynthesis, growth and cell composition of the cyanobacterium *Spirulina*
522 *platensis* (Arthrospira). J Appl Phycol 10:461–469
523 Gordillo FJL, Niell FX, Figueroa FL (2001) Non-photosynthetic enhancement of growth by high CO_2
524 level in the nitrophilic seaweed *Ulva rigida* C. Agardh (Chlorophyta). Planta 213:64–70
525 Gordillo FJL, Figueroa FL, Niell FX (2003) Photon- and carbon-use efficiency in *Ulva rigida* at different
526 CO_2 and N levels. Planta 218:315–322
527 Gordillo FJL, Aguilera J, Jimenez C (2006) The response of nutrient assimilation and biochemical
528 composition of Arctic seaweeds to a nutrient input in summer. J Exp Bot 57:2661–2671
529 Gran G (1952) Determination of the equivalence point in potentiometric titrations. Part II. Analyst
530 77:661–671
531 Gutow L, Rahman MM, Bartl K, Saborowski R, Bartsch I, Wiencke C (2014) Ocean acidification affects
532 growth but not nutritional quality of the seaweed *Fucus vesiculosus* (Phaeophyceae, Fucales). J
533 Exp Mar Biol Ecol 453:84–90
534 Hall-Spencer JM, Rodolfo-Metalpa R, Martin S, Ransome E, Fine M, Turner SM, Rowley SJ, Tedesco D,
535 Buia MC (2008) Volcanic carbon dioxide vents reveal ecosystem effects of ocean acidification.
536 Nature 454:96–99
537 Henley WJ, Dunton KH (1997) Effects of nitrogen supply and continuous darkness on growth and
538 photosynthesis of the Arctic kelp *Laminaria solidungula*. Limnol Oceanogr 42:209–216
539 Hennon GMM, Quay P, Morales RL, Swanson LM, Armbrust EV (2014) Acclimation conditions modify
540 physiological response of the diatom *Thalassiosira pseudonana* to elevated CO_2 concentrations
541 in a nitrate-limited chemostat. J Phycol 50:243–253
542 Hop H, Pearson T, Hegseth EN, Kovacs KM, Wiencke C, Kwasniewski S, Eiane K, Mehlum F, Gulliksen
543 B, Wlodarska-Kowalczuk M, Lydersen C, Weslawski JM, Cochrane S, Gabrielsen GW, Leakey
544 RJG, Lønne OJ, Zajaczkowski M, Falk-Petersen S, Kendall M, Wängberg S-A, Bischof K,
545 Voronkov AY, Kovaltchouk NA, Wiktor J, Poltermann M, di Prisco G, Papucci C, Gerland S
546 (2002) The marine ecosystem of Kongsfjorden, Svalbard. Polar Res 21:167–208.
547 Hop H, Wiencke C, Vögele B, Kovaltchouk NA (2012) Species composition, zonation and biomass of
548 marine benthic macroalgae in Kongsfjorden, Svalbard. Bot Mar 55:399–414
549 Hopkinson BM, Xu Y, Shi D, McGinn PJ, Morel FMM (2010) The effect of CO_2 on the photosynthetic
550 physiology of phytoplankton in the Gulf of Alaska. Limnol Oceanogr 55:2011–2024
551 Hurd CL, Hepburn CD, Currie KI, Raven JA, Hunter KA (2009) Testing the effects of ocean acidification
552 on algal metabolism: recommendations for experimental designs. J Phycol 45:1236–1251
553 IPCC (2013) The Intergovernmental Panel on Climate Change. Climate Change 2013: The physical
554 science basis. Summary for policymakers. Cambridge University Press, Cambridge pp 24–25

555 Israel A, Katz S, Dubinsky Z, Merrill JE, Friedlander M (1999) Photosynthetic inorganic carbon
556 utilization and growth of *Porphyra linearis* (Rhodophyta). J Appl Phycol 11:447–53
557 Israel A, Hophy M (2002) Growth, photosynthetic properties and Rubisco activities and amounts of
558 marine macroalgae grown under current and elevated seawater CO_2 concentrations. Glob Change
559 Biol 8:831–840
560 Korb RE, Gerard VA (2000) Effects of concurrent low temperature and low nitrogen supply on polar and
561 temperate waters. Mar Ecol Prog Ser 198:73–82
562 Kremer BP, Küppers U (1977) Carboxylating enzymes and pathway of photosynthetic carbon
563 assimilation in different marine algae–evidence for the C_4 pathway? Planta 133:191–6
564 Kristensen E, Andersen F (1987) Determination of organic carbon in marine sediments: a comparison of
565 two CHN-analyzer methods. J Exp Mar Bio Ecol 109:15–23
566 Kübler JE, Johnston AM, Raven JA (1999) The effects of reduced and elevated CO_2 and O_2 on the
567 seaweed *Lomentaria articulata*. Plant Cell Environ 22:1303–1310
568 Lüning K (1985) Meeresbotanik. Verbreitung, Ökophysiologie und Nutzung der marinen Makroalgen.
569 Thieme Verlag Stuttgart, pp 375
570 Lüning K (1991) Circannual growth rhythm in a brown alga, *Pterygophora californica*. Bot Acta
571 104:157–162
572 Maberly SC, Raven JA, Johnston AM (1992) Discrimination between ^{12}C and ^{13}C by marine plants.
573 Oecologia 91:481–492
574 Mague TH, Friberg E, Hughes DJ, Morris I (1980) Extracellular release of carbon by marine
575 phytoplankton: a physiological approach. Limnol. Oceanogr. 25:262-279
576 Matsuda Y, Hara T, Colman B (2001) Regulation of the induction of bicarbonate uptake by dissolved
577 CO_2 in the marine diatom *Phaeodactylum tricornutum*. Plant Cell Environ 24:611–620
578 Mehrbach C, Culberson CH, Hawley JE, Pytkowicz RM (1973) Measurement of the apparent
579 dissociation constants of carbonic acid in seawater at atmospheric pressure. Limnol Oceanogr
580 18:897–907
581 Mercado JM, Gordillo FJL, Niell FX, Figueroa FL (1999) Effects of different levels of CO_2 on
582 photosynthesis and cell components of the red alga *Porphyra leucosticta*. J Appl Phycol 11:455–
583 461
584 Mercado JM, de los Santos CB, Pérez-Lloréns JL, Vergara JJ (2009) Carbon isotopic fractionation in
585 macroalgae from Cádiz Bay (Southern Spain): Comparison with other bio-geographic regions.
586 Estuar Coast Shelf Sci 85:449–458
587 Moulin P, Andria JR, Axelsson L, Mercado JM (2011) Different mechanisms of inorganic carbon
588 acquisition in red macroalgae (Rhodophyta) revealed by the use of TRIS buffer. Aquat Bot
589 95:31–38
590 O'Leary MH, Madhavan S, Paneth P (1992) Physical and chemical basis of carbon isotope fractionation
591 in plants. Plant Cell Environ 15:1099–1104
592 Olabarria C, Arenas F, Viejo RM, Gestoso I, Vaz-Pinto F, Incera M, Rubal M, Cacabelos E, Veiga P,
593 Sobrino C (2013) Response of macroalgal assemblages from rockpools to climate change:
594 effects of persistent increase in temperature and CO_2. Oikos 122:1065–1079

595 Olischläger M, Wiencke C (2013) Ocean acidification alleviates low-temperature effects on growth and
596 photosynthesis of the red alga *Neosiphonia harveyi* (Rhodophyta). J Exp Bot 64:5587–5597
597 Ormerod JG (1983) The carbon cycle in aquatic ecosystems. In: Slater JH, Whittenbury R, Wimpenny
598 JWT (eds) Microbes in their natural environments. Cambridge University Press, Cambridge, pp
599 463–482
600 Provasoli L (1968) Media and prospects for the cultivation of marine algae. In: Watanabe A, Hattori A
601 (eds) Cultures and Collections of Algae. Proceedings of the U.S.-Japan Conference, Hakone
602 1966. Japanese Society for Plant Physiology, Tokyo, pp 63–75
603 Raven JA, Johnston AM, Kübler JE, Korb R, Mcinroy SG, Handley LL, Scrimgeour CM, Walker DI,
604 Beardall J, Vanderklift M, Fredriksen S, Dunton KH (2002) Mechanistic interpretation of carbon
605 isotope discrimination by marine macroalgae and seagrasses. Funct Plant Biol 29:335–78
606 Raven JA, Beardall J (2003) Carbon acquisition mechanisms of algae: carbon dioxide diffusion and
607 carbon dioxide concentrating mechanisms. In: Larkum AW, Douglas SE, Raven JA (eds)
608 Photosynthesis in algae. Advances in Photosynthesis and Respiration. Vol. 14. Kluwer
609 Academic Publishers, The Netherlands, pp 225–244
610 Riebesell U, Schulz KG, Bellerby RGJ, Botros M, Fritsche P, Meyerhöfer M, Neill C, Nondal G,
611 Oschlies A, Wohlers J, Zöllner E (2007) Enhanced biological carbon consumption in a high CO_2
612 ocean. Nature 450:545–549
613 Robbins LL, Hansen ME, Kleypas JA, Meylan SC (2010) CO2calc—A user-friendly seawater carbon
614 calculator for Windows, Max OS X, and iOS (iPhone): U.S. Geological Survey Open-File
615 Report 2010–1280, 17 p.
616 Roleda MY, Hurd CL (2012) Seaweed Responses to Ocean Acidification. In: Wiencke C, Bischof K.
617 (eds.) Seaweed Biology, Ecological Studies 219. Springer-Verlag, pp 407–431
618 Russell BD, Thompson JAI, Falkenberg LJ, Connell SD (2009) Synergistic effects of climate change and
619 local stressors: CO_2 and nutrient-driven change in subtidal rocky habitats. Glob Change Biol
620 15:2153–2162
621 Satoh A, Kurano N, Senger H, Miyachi S (2002) Regulation of energy balance in photosystems in
622 response to changes in CO_2 concentrations and light intensities during growth in extremely high-
623 CO_2-tolerant green microalgae. J Plant Cell Physiol 43:440–451
624 Schaffelke B, Lüning K (1994) A circannual rhythm controls seasonal growth in the kelps *Laminaria*
625 *hyperborea* and *Laminaria digitata* from Helgoland (North Sea). Eur J Phycol 29:49–56
626 Schreiber U, Schliwa U, Bilger W(1986) Continuous recording of photochemical and non-photochemical
627 chlorophyll fluorescence quenching with a new type of modulation fluorometer. Photosynth Res
628 10:51–62
629 Sharp JH (1977) Excretion of organic matter by marine phytoplankton: do healthy cells do it? Limnol
630 Oceanogr 22:381–399
631 Sobrino C, Segovia M, Neale P, Mercado JM, García-Gómez C, Kulk G, Lorenzo MR, Camarena T, Van
632 de Poll W, Spilling K (2014) Interactive effects of solar radiation, CO_2 and nutrient enrichment
633 on cell viability and organic carbon excretion of coastal phytoplankton. Aquat Biol. doi:
634 10.3354/ab00590

635 Steeman-Nielsen E (1952) The use of radioactive carbon (^{14}C) for measuring organic production in the
636 sea. J Cons Int Explor Mer 18:117–140
637 Steinacher M, Joos F, Frölicher TL, Plattner G-K, Doney SC (2009) Imminent ocean acidification in the
638 Arctic projected with the NCAR global coupled carbon cycle-climate model. Biogeosciences
639 6:515–533
640 Suárez-Álvarez S, Gómez-Pinchetti JL, García-Reina G (2012) Effects of increased CO_2 levels on
641 growth, photosynthesis, ammonium uptake and cell composition in the macroalga *Hypnea*
642 *spinella* (Gigartinales, Rhodophyta). J Appl Phycol 24:815–823
643 Swanson AK, Fox CH (2007) Altered kelp (Laminariales) phlorotannins and growth under elevated
644 carbon dioxide and ultraviolet-B treatments can influence associated intertidal food webs. Glob
645 Change Biol 13:1696–1709
646 Wassmann P, Duarte CM, Agustí S, Sejr MK (2011) Footprints of climate change in the Arctic marine
647 ecosystem. Glob Change Biol 17:1235–1249
648 Weiss RF (1974) Carbon dioxide in water and seawater: the solubility of a non-ideal gas. Mar Chem
649 2:203-215
650 Wiencke C, Vögele B, Kovaltchouk NA, Hop H (2004) Species composition and zonation of marine
651 benthic macroalgae at Hansneset in Kongsfjorden, Svalbard. Ber Polarforsch Meeresforsch
652 492:55–62
653 Wiencke C, Clayton MN, Gómez I, Iken K, Lüder UH, Amsler CD, Karsten U, Hanelt D, Bischof K,
654 Dunton K (2007) Life strategy, ecophysiology and ecology of seaweeds in polar waters. Rev
655 Environ Sci Biotechnol 6:95–126
656 Wiencke C, Gómez I, Dunton K (2011) Phenology and seasonal physiological performance in polar
657 seaweeds. In: Wiencke C (ed) Biology of polar benthic algae. de Gruyter, Berlin, pp 181–194
658 Wood AM, Van Valen LM (1990) Paradox lost? On the reléase of energy rich compounds by
659 phytoplankton. Mar Microb Food Webs 4:103–116
660 Wu Y, Gao K, Riebesell U (2010) CO_2-induced seawater acidification affects physiological performance
661 of the marine diatom *Phaeodactylum tricornutum*. Biogeosciences 7:2915–2923
662 Xu ZG, Zou DH, Gao KS (2010) Effects of elevated CO_2 and phosphorus supply on growth,
663 photosynthesis and nutrient uptake in the marine macroalga *Gracilaria lemaneiformis*
664 (Rhodophyta). Bot Mar 53:123–9
665 Yang G, Gao K (2012) Physiological responses of the marine diatom *Thalassiosira pseudonana* to
666 increased pCO_2 and seawater acidity. Mar Environ Res 79:142–151
667 Zou DH (2005) Effects of elevated atmospheric CO_2 on growth, photosynthesis and nitrogen metabolism
668 in the economic brown seaweed, *Hizikia fusiforme* (Sargassaceae, Phaeophyta). Aquaculture
669 250:726–735
670 Zou D, Gao K (2009) Effects of elevated CO_2 on the red seaweed *Gracilaria lemaneiformis* (Gigartinales,
671 Rhodophyta) grown at different irradiance levels. Phycologia 48:510–7
672 Zou D, Gao K, Luo H (2011a) Short- and long-term effects of elevated CO_2 on photosynthesis and
673 respiration in the marine macroalga *Hizikia fusiformis* (Sargassaceae, Phaeophyta) grown at low
674 and high N supplies. J Phycol 47:87−97

675 Zou D, Gao K, Xia J (2011b) Dark respiration in the light and in darkness of three marine macroalgal
676 species grown under ambient and elevated CO_2 concentrations. Acta Oceanol 30:106−112

Figures

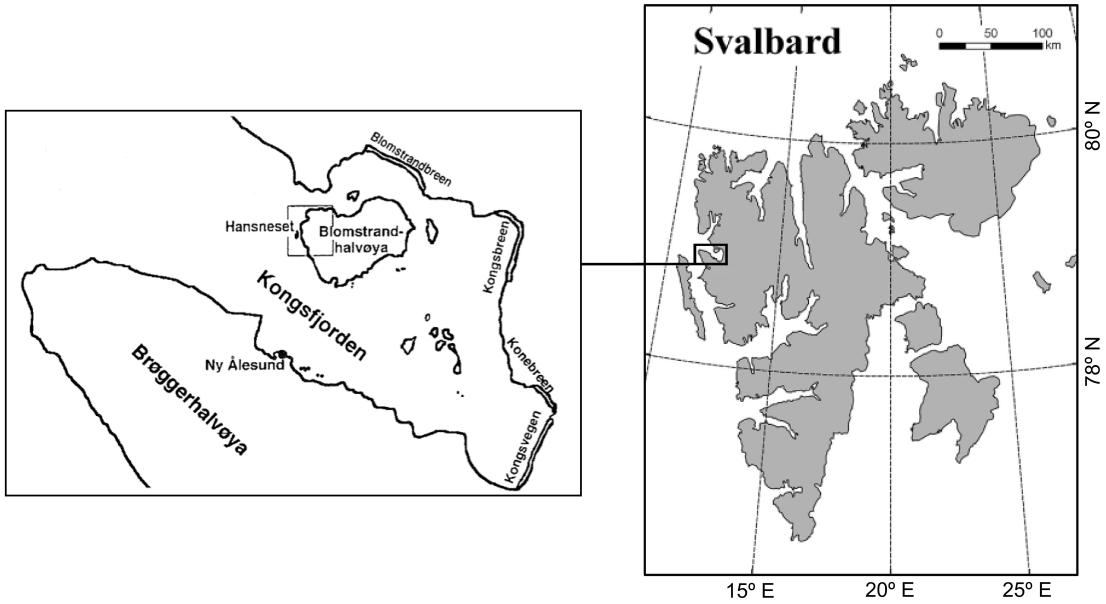

Figure 1. Map of Svalbard archipielago (right) and the Kongsfjord on Spitsbergen (left), with an indication of the collecting site (Hansneset).

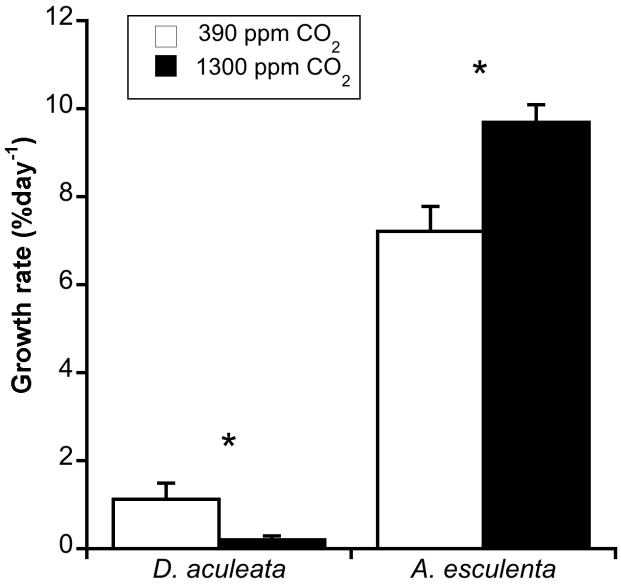

Figure 2. Growth rate expressed as % d^{-1} (mean and SD, n = 4) of *Desmarestia aculeata* and *Alaria esculenta* during 7 days of culture at 390 and 1300 ppm CO_2. Statistically significant differences between both CO_2 conditions for each species are indicated by an asterisk ($P < 0.05$).

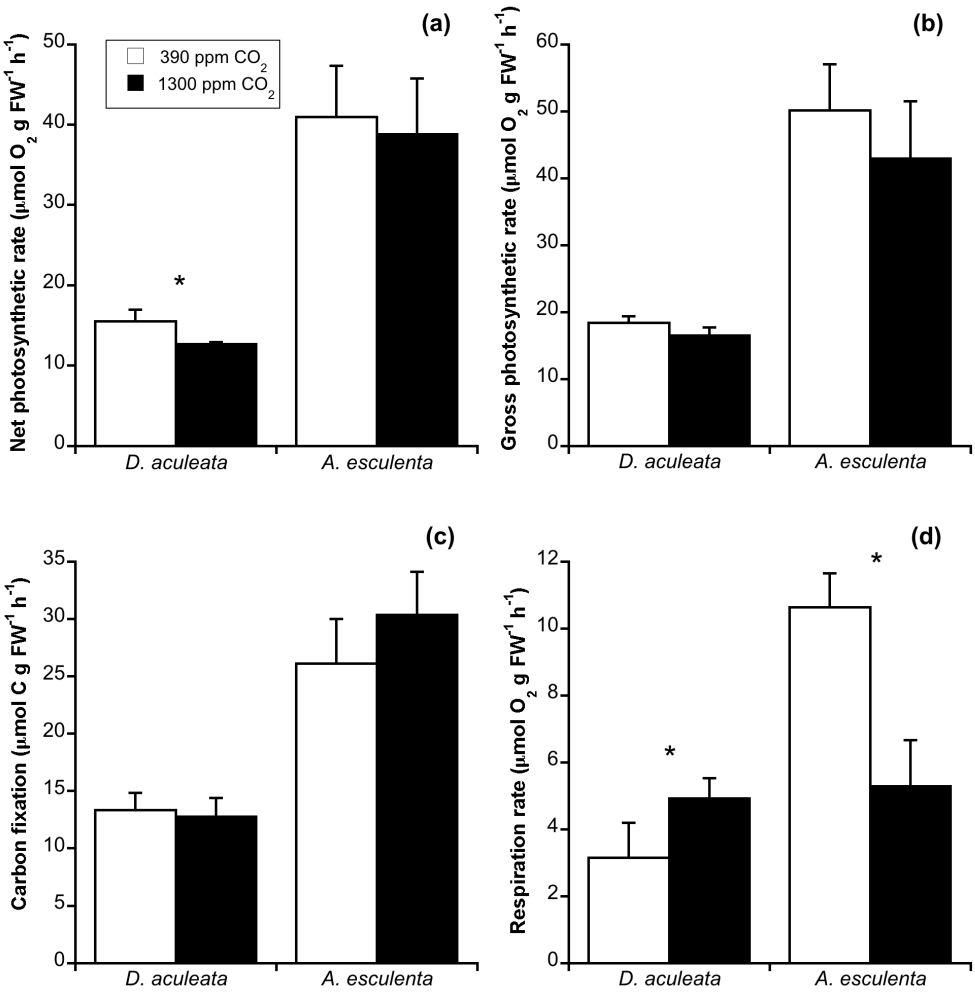

Figure 3. Net photosynthetic rate (a), gross photosynthetic rate (b), and dark respiration rate (d) measured by oxygen evolution, and photosynthetic rate measured by ^{14}C fixation (c) of *Desmarestia aculeata* and *Alaria esculenta* after 7 days of culture at 390 and 1300 ppm CO_2. Statistically significant differences between both CO_2 conditions for each species are indicated by asterisk ($P < 0.05$) (mean and SD, n = 4).

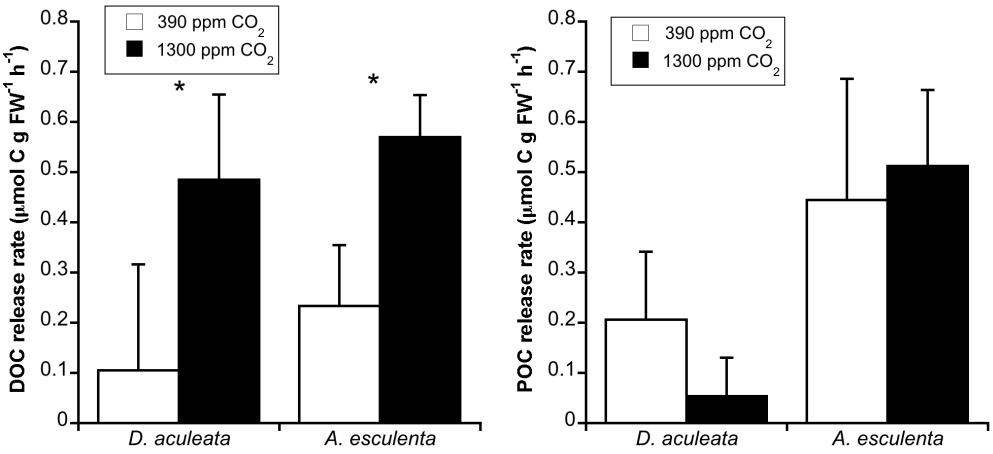

Figure 4. Dissolved organic carbon (DOC) and particulate organic carbon (POC) release rate of *Desmarestia aculeata* and *Alaria esculenta* during 7 days of culture at 390 and 1300 ppm CO_2. Significant differences between both CO_2 conditions for each species are indicated by asterisk ($P < 0.05$) (mean and SD, n = 4).

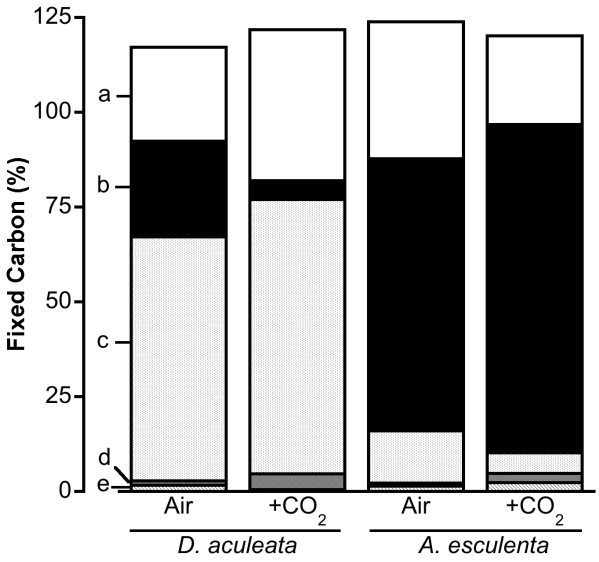

Figure 5. Distribution of total fixed carbon during the 7 days of culture at both CO_2 conditions among different cellular processes, expressed as a percentage. *a* fixed carbon lost by respiration; *b* invested in new biomass production (growth); *c* accumulated in storage biomolecules; *d*, *e* organic carbon released and found in the medium in dissolved (DOC) and particulate (POC) form, respectively.

Table 1. Seawater carbonate system (SWCS) over the experimental period in *Desmarestia aculeata* and *Alaria esculenta*. Values are the mean ± standard deviation (SD). All replicates were analysed every 2-3 days (n = 4).

	D. aculeata		***A. esculenta***	
	390 ppm CO_2	**1300 ppm CO_2**	**390 ppm CO_2**	**1300 ppm CO_2**
pH_{NBS}	8.17 ± 0.04	7.72 ± 0.02	8.19 ± 0.07	7.72 ± 0.03
pCO_2 (µatm)	410 ± 52	1252 ± 30	395 ± 27	1300 ± 36
CO_2 (µmol kg SW^{-1})	23 ± 3	69 ± 2	22 ± 1	71 ± 2
HCO_3^- (µmol kg SW^{-1})	2265 ± 56	2453 ± 10	2280 ± 25	2462 ± 15
CO_3^{2-} (µmol kg SW^{-1})	123 ± 9	47 ± 1	129 ± 9	45 ± 1
DIC (µmol kg SW^{-1})	2410 ± 49	2569 ± 10	2431 ± 27	2578 ± 15
TA (µmol kg SW^{-1})	2566 ± 34	2568 ± 9	2595 ± 35	2573 ± 17

DIC, dissolved inorganic carbon; TA, total alkalinity.

Table 2. Photosynthetic parameters calculated from Chlorophyll *a* fluorescence measurements (mean ± SD, n = 4) of *Desmarestia aculeata* and *Alaria esculenta* after 7 days of culture at either 390 or 1300 ppm CO_2. ETR_{30} represents the electron transport rate at an irradiance of 30 µmol photons m^{-2} s^{-1} (measured with the quantum flat head PAR sensor), similar to culture conditions. Significant differences between both CO_2 conditions for each species are indicated by an asterisk ($P < 0.05$).

	D. aculeata		***A. esculenta***	
	390 ppm CO_2	**1300 ppm CO_2**	**390 ppm CO_2**	**1300 ppm CO_2**
ETR_{30} (µmol e^- m^{-2} s^{-1})	7.3 ± 0.48	6.23 ± 0.33 *	3.07 ± 0.6	4.55 ± 0.6 *
ETR_{max} (µmol e^- m^{-2} s^{-1})	21.01 ± 2.38	14.9 ± 2.32 *	3.21 ± 0.71	5.14 ± 0.64 *
α (e^- $photons^{-1}$)	0.23 ± 0.04	0.24 ± 0.07	0.17 ± 0.02	0.23 ± 0.04 *
E_k (µmol photons m^{-2} s^{-1})	80.1 ± 3.2	78 ± 18.1	19.1 ± 1.9	23.8 ± 2.5 *
E_{0pt} (µmol photons m^{-2} s^{-1})	306 ± 78	272 ± 27	38.2 ± 3.9	47.7 ± 5.1 *
F_v/F_m	0.72 ± 0.03	0.72 ± 0.04	0.67 ± 0.03	0.68 ± 0.01

Table 3. The photosynthetic quotient (PQ), calculated as gross oxygen production divided by ^{14}C fixation, of *Desmarestia aculeata* and *Alaria esculenta* after 7 days of culture at 390 and 1300 ppm CO_2. Significant differences between both CO_2 conditions for each species are indicated by an asterisk ($P < 0.05$) (mean ± SD, n = 4).

D. aculeata		***A. esculenta***	
390 ppm CO_2	**1300 ppm CO_2**	**390 ppm CO_2**	**1300 ppm CO_2**
1.38 ± 0.13	1.30 ± 0.15	1.92 ± 0.40	1.41 ± 0.33 *

Table 4. Elemental composition of total C, total N, atomic C:N ratio, the corrected ^{13}C isotopic discrimination in the algal samples ($\delta^{13}C_{alga}$) and FW:DW ratio (mean ± SD, n = 4) of *Desmarestia aculeata* and *Alaria esculenta* after 7 days of culture at 390 and 1300 ppm CO_2. Significant differences between both CO_2 conditions for each species are indicated by an asterisk ($P < 0.05$).

	D. aculeata		***A. esculenta***	
	390 ppm CO_2	**1300 ppm CO_2**	**390 ppm CO_2**	**1300 ppm CO_2**
Total C (% DW)	35.72 ± 1.25	35.86 ± 1.21	32.84 ± 0.23	30.64 ± 1.01 *
Total N (% DW)	2.17 ± 0.11	1.97 ± 0.05 *	3.48 ± 0.23	3.92 ± 0.1 *
C:N ratio	19.29 ± 1.39	21.26 ± 0.63	11.04 ± 0.73	9.12 ± 0.36 *
$\delta^{13}C_{alga}$ (‰)	-19.22 ± 2.06	-23.47 ± 2.25 *	-21.84 ± 1.75	-28.66 ± 1.49 *
FW:DW ratio	3.93 ± 0.5	3.65 ± 0.13	4.41 ± 0.07	5.19 ± 0.21 *